Proposal of Carburization Depth Inspection of Both Surface and Opposite Side on Steel Tube Using 3D Nonlinear FEM in Consideration of the Carbon Concentration

Saijiro Yoshioka(✉) and Yuji Gotoh

Department of Mechanical and Energy Systems Engineering,
Faculty of Engineering, Oita University, 700 Dannoharu, Oita 870-1192, Japan
vl5fl003@oita-u.jp

Abstract. In the steel tube of a heating furnace inside an oil-refining plant, its both surface and opposite side is carburized. If these carburization depths are increased, the steel tube will be exploded suddenly and a big accident may occur. Therefore, the inspection of these carburization depths is important. The conductivity of the layer with carburization is larger than the layer without carburization in the steel, and its permeability is smaller than the layer without carburization. Therefore, the estimation of both carburization depths is possible by using the differences of these electromagnetic properties. In this paper, the new technique of measuring the both depths by using two kinds of alternating magnetic field is proposed. The both depths are obtained by evaluating the flux density in layers with and without carburization steel tube using the 3-D non-linear FEM. It is shown that the inspection of both depths is possible by using the differential electromagnetic characteristics.

Keywords: Electromagnetic non-destructive inspection · Carburization steel tube · Both surface and opposite side depth · 3-D finite element method

1 Introduction

In recent years, the necessity for inspection of the deteriorated oil-refining plant is increased. In particular, the non-destructive inspection of a heating furnace steel tube in the plant is important. In the steel tube, its both surface and opposite side are carburized. If these carburization depths are increased, the steel tube will be exploded suddenly and a big accident may occur. Therefore, the inspection for these depths is important. The conductivity of the layer with carburization is larger than the layer without carburization in the steel tube, and its permeability is smaller than the layer without carburization [1]. Then, the evaluation of these depths is possible by detecting the difference of these electromagnetic characteristics [2–5].

In this paper, the electromagnetic inspection method for these carburization depths is proposed. In this method, the alternating magnetic field of the two kinds of exciting frequency using one sensor is applied to the examined steel tube. These both depths are

N. Kubota et al. (Eds.): ICIRA 2016, Part I, LNAI 9834, pp. 739–748, 2016.
DOI: 10.1007/978-3-319-43506-0_63

obtained by evaluating the flux density in layers with and without carburization inside steel tube using the 3-D nonlinear FEM. In addition, the experimental verification is also carried out.

2 Inspection Model and Method of Analysis

2.1 Measurement of Electromagnetic Properties With and Without Carburization Steel

Figure 2 shows the example of measurement result of carbon concentration inside steel tube using electron probe-micro analysis (EPMA) when the surface carburization depth d_s and the opposite side depth d_o are equal to 1 mm and 2.5 mm, respectively. The domain that the carbon concentration is more than 0.27 % is defined as the carburization layer. The figure denotes that the carbon concentration in the carburization layer is nonlinearly distributed from about 3.8 % to 0.27 % (layer without carburization).

The macroscopic magnetization curves of the rectangular specimens with and without carburization steel (STFA26) are measured using a magnetization equipment as shown in Fig. 2. The average carbon concentration in the rectangular specimen without carburization is 0.27 %. The rectangular specimen with carburization is a full carburized material, and the average carbon concentration is 3.8 %. A rectangular specimen of the steel is placed between magnetic yokes, and magnetized by magnetic field of 0.1 Hz (The minimum exciting frequency in the magnetizing equipment). The flux density in the specimen is measured using a search coil (B coil) wound around the specimen. The magnetic field strength is measured using a thin search coil (H coil) arranged on the specimen [4]. The output voltages of these search coils are amplified with a small-signal amplifier with noise filter, and calculated by the integration of a computer. Figure 3 shows *B-H* curves [6] of the steel tube with and without carburization layer. The carbon concentration in the carburization layer is equal to 3.8 %.

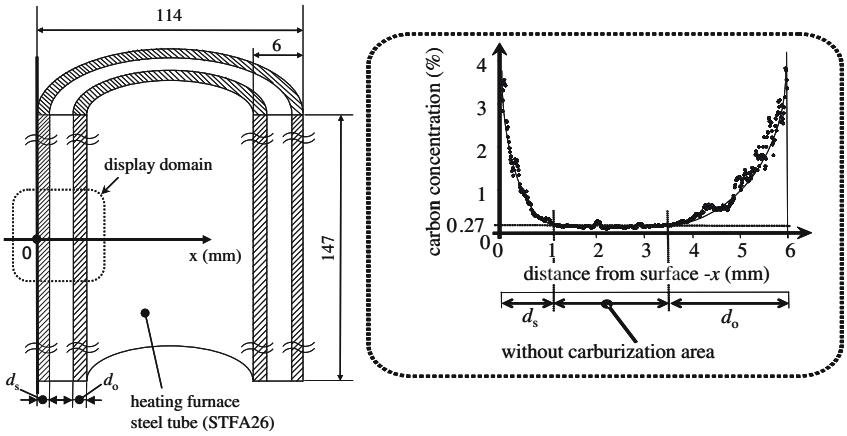

Fig. 1. Distribution of carbon concentration using electron probe-micro analysis (EPMA) when d_s and d_o are equal to 1 mm and 2.5 mm.

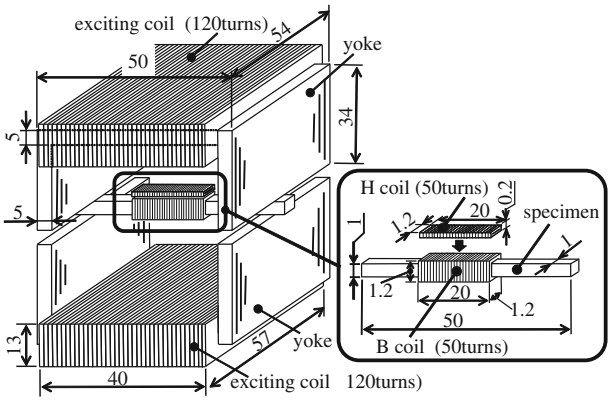

Fig. 2. Magnetization equipment for measuring magnetic properties of the rectangular speci mens with and without carburization steel (STFA26 steel, exciting frequency: 0.1 Hz)

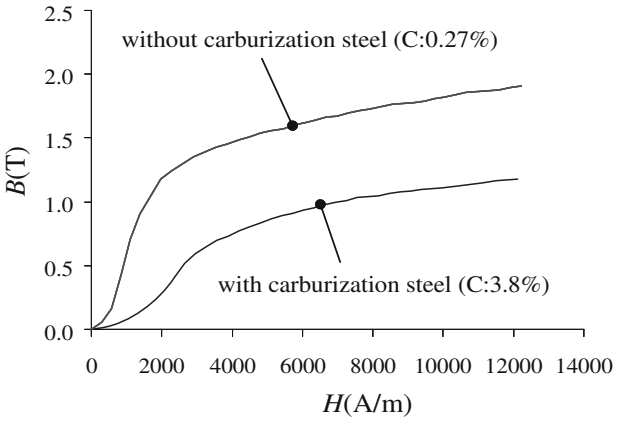

Fig. 3. *B-H* curves of with and without carburization steel (STFA26 steel).

The figure denotes that the permeability in the steel is decreased by the carburization. This is, because the magnetic property of the carburized domain is changed to the structure of strain crystal. Since many lattice defects are generated in the strain crystal, the magnetic wall motion is interfered by the lattice defects [1]. The conductivity of the steel with and without carburization is measured using the Kelvin bridge circuit. Figure 4 shows the conductivities of the steel with and without carburization. The figure denotes that the conductivity of the steel is decreased with the carburization. This is, because it is thought that the conductivity is increased since the carbon permeated into the steel. The conductivity of the steel without carburization is about 1.28 times of that of the steel with carburization.

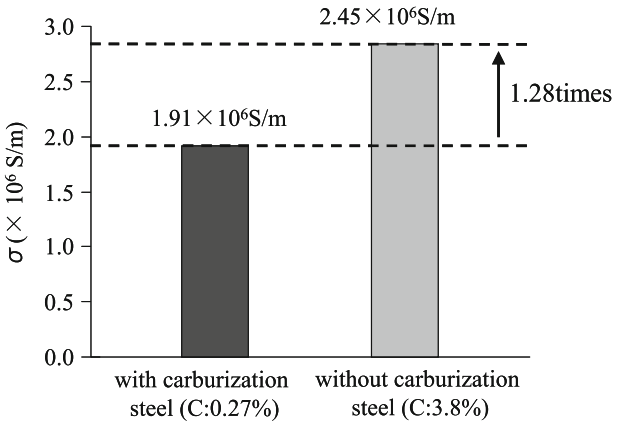

Fig. 4. Conductivities of with and without carburization steel (STFA26 steel).

2.2 Electromagnetic Inspection Model

Figure 5 shows the proposed model for inspecting the both surface and opposite side of the carburization depth in steel tube. This model is composed of the yokes (lamination of silicon steel plates) for ac (alternating) magnetic field and a search coil. As for the

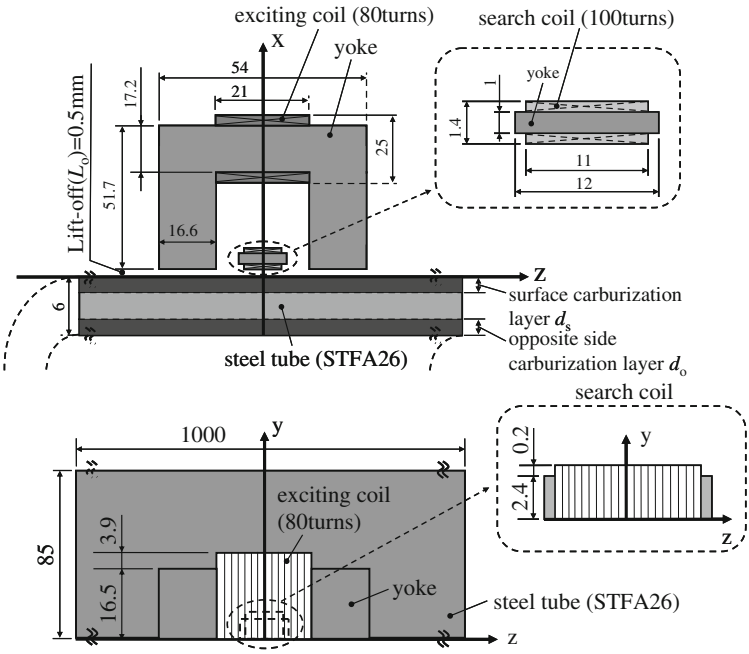

Fig. 5. Proposed model for inspecting carburization depth of both the surface (d_s) and the opposite side (d_o) in steel tube.

search coil in this sensor, the z-direction flux density (B_z) of the magnetic field on the surface of the steel tube is detected. The distance (lift-off: L_o) between the sensor and the surface of steel tube is equal to 0.5 mm. The exciting ampere-turns is 16AT. The exciting frequency of 500 Hz and 15 Hz by one electromagnetic sensor is used to inspect both surface and opposite side of carburized layer in the steel tube.

2.3 3-D Electromagnetic FEM Analysis Method

3-D FEM using the 1st order hexahedral edge element is applied. The flux and eddy current are analyzed by the step-by-step method taking account of the non-linearity of the steel tube. Moreover, an initial magnetization curve of the magnetic yoke is also taken into consideration, but the eddy current is neglected. In order to get the steady state result, the calculation is carried out during 3 periods (=96 steps). The basic equation of eddy current analysis using the $\boldsymbol{A}$-ϕ method is given by

$$rot(vrot\boldsymbol{A}) = \boldsymbol{J}_0 - \sigma\left(\frac{\partial \boldsymbol{A}}{\partial t} + grad\phi\right) \tag{1}$$

$$div\left\{-\sigma\left(\frac{\partial \boldsymbol{A}}{\partial t} + grad\phi\right)\right\} = 0 \tag{2}$$

where $\boldsymbol{A}$ is the magnetic vector potential, ϕ is the scalar potential, v is the reluctivity, $\boldsymbol{J_o}$ is the current density and σ is the conductivity.

The carbon concentration is changed non-linearly as it approaches to without carburization layer. Therefore, the numerical value of B-H curves and conductivity are different by with carburization layer location. Analysis is obtained by interpolating the carbon concentration using Fig. 1, and performs the nonlinear calculation. For non-linear calculations is calculated by changing the B-H curves to v-B^2 curves of the magnetic resistivity and flux density. Figure 6 shows v-B^2 curves of carbon concentration 0.27 %

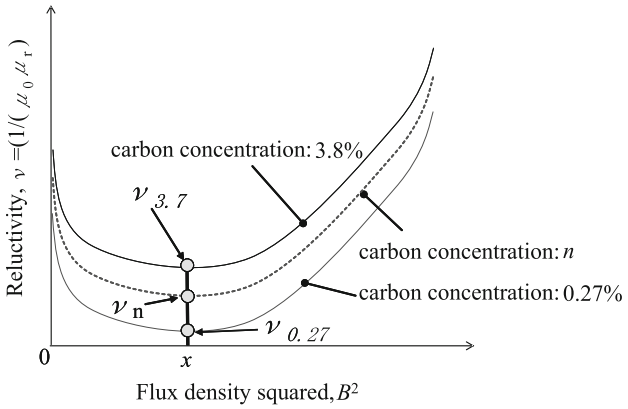

Fig. 6. v-B^2 curves of with and without carburization steel (STFA26 steel).

and 3.8 % used non-linear electromagnetic analysis. It performs the calculation of the *B*-*H* curves and conductivity using this interpolation method for all elements in the with carburization layer.

3 Inspection of Carburization Depth of Both the Surface and the Opposite Side in Steel Tube

In this research, the carburizations depths of both the surface d_s and the opposite side d_o are inspected by the difference of these electromagnetic characteristics using two kinds of alternating magnetic fields.

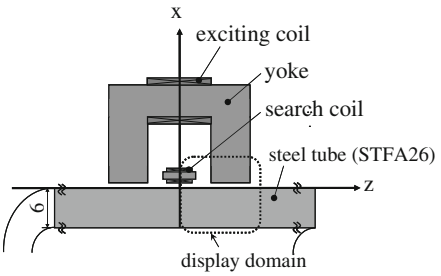

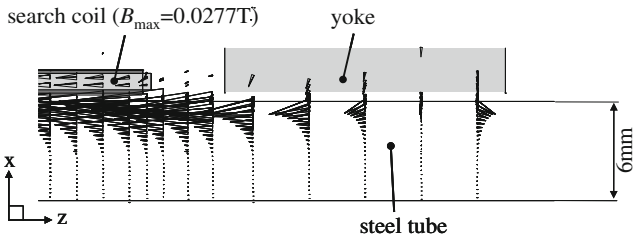

(a) surface carburization depth d_s=0mm (B_{max}=0.096T)

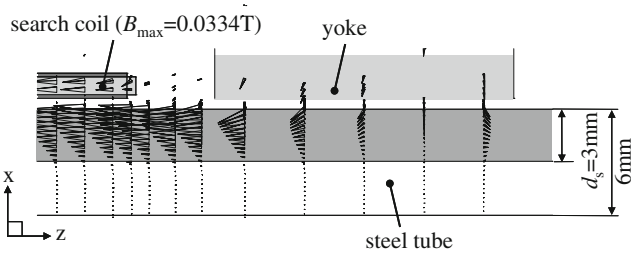

(b) surface carburization depth d_s=3mm (B_{max}=0.036T)

Fig. 7. Distribution of flux density in steel tube with and without surface carburization (500 Hz, 16AT).

3.1 Inspection of Surface Carburization Depth

At first, an alternating magnetic field of 500 Hz is impressed to the steel tube, and the surface carburization depth is inspected. Figure 7 shows the distribution of flux density in the steel tube when the surface carburization depth d_s is equal to 0 mm and 3 mm, respectively. These figures illustrate that the flux density is distributed on the surface of the steel tube by a skin effect, since exciting frequency is high as 500 Hz. Then, the maximum flux density in steel tube is decreased when the surface carburization depth d_s is increased since the permeability in the carburization layer is lower than that of the non-carburization layer.

Figure 8 shows the effect of the change of flux density B_z in a search coil by the 3-D nonlinear FEM when only the surface depth d_s is changed. The figure denotes the rate of change from the measured value B_z of the steel tube without the carburization. The figure illustrates that B_z is increased when the surface depth d_s is increased. This is because, the leakage flux on surface of the steel tube is increased when the surface depth d_s is increased, since the permeability of carburization layer is lower than the non-carburization layer [2]. Therefore, only the surface depth d_s is inspected using the high exciting frequency of 500 Hz as shown in Fig. 8.

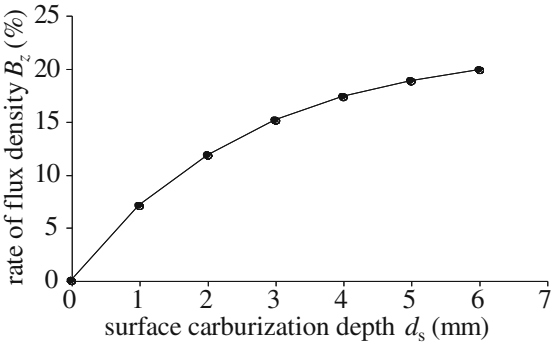

Fig. 8. Effect of the change of flux density B_z in a search coil by the 3-D nonlinear FEM when only the surface depth d_s is changed. (500 Hz, 16AT, calculated).

3.2 Inspection of Opposite Side Carburization Depth

Next, an alternating magnetic field of 15 Hz is impressed to the steel tube, and the opposite side carburization depth d_o is inspected. Figure 9 shows the distribution of flux density in the steel tube when the opposite side carburization depth d_o is equal to 0 mm and 3 mm, respectively. These figures illustrate that the flux density is distributed to the deep domain near the opposite side of steel tube when the opposite side depth d_o is equal to 0 mm, since exciting frequency is low as 15 Hz. However, the flux density is distributed in surface steel tube when the opposite side depth d_o is increased since the permeability in the carburization layer is lower than that the non-carburization layer.

Figure 10 shows the effect of change of flux density B_z in a search coil by the 3-D nonlinear magnetic FEM when only the opposite side depth d_o is changed. The figure

denotes the rate of change from the measured value B_z of the steel tube without the carburization. Moreover, the rate of flux density B_z for each opposite side depth d_o is also shown when each surface depth d_s is in constant depth. The figure illustrates that B_z is increased when the opposite side depth d_o is increased. This is because, the leakage flux on surface of the steel tube is increased, since the flux density in surface steel tube is increased when the opposite side depth d_o is increased as shown in Fig. 9. The opposite side depth d_o is inspected using linear interpolation of the curves corresponding to each surface depth d_s as shown in Fig. 10, since the surface depth d_s was inspected using the high exciting frequency of 500 Hz as shown in Fig. 8.

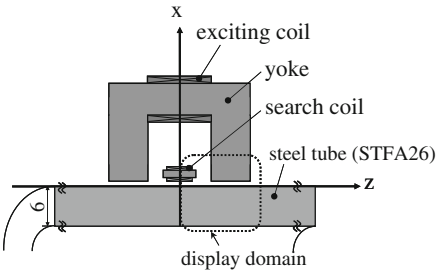

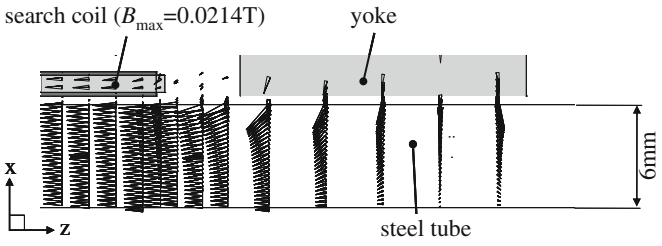

(a) opposite side carburization depth d_o=0mm (B_{max}=0.047T)

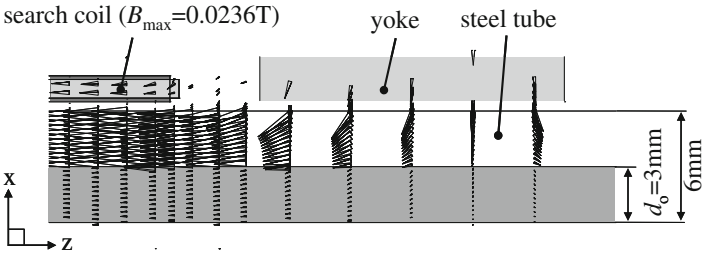

(b) opposite side carburization depth d_o=3mm (B_{max}=0.056T)

Fig. 9. Distribution of flux density in steel tube with and without opposite side carburization (15 Hz, 16AT).

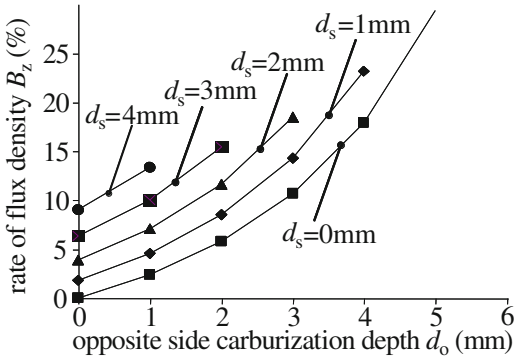

Fig. 10. Effect of change of flux density B_z in a search coil by the 3-D nonlinear FEM when only the opposite side depth do is changed(15 Hz, 16AT, calculated).

4 Verification Evaluation by Actual Carburized Steel Tube in the Oil-Refining Plant

The surface and opposite sides of carburization depth in actual steel tube inside the oil-refining plant are inspected by the proposed method. The heating furnace steel tube which continued being used for 30 years inside the oil-refining plant in Japan was inspected. Table 1 shows the inspection results of the surface and opposite sides of carburization depth. The domain that the carbon concentration is more than 0.27 % by using EPMA is defined as the actual carburization depth. In the proposed method, the carburization depth of the surface and opposite side is searched by the linear interpolation of the calculated values as shown in Figs. 8 and 10. This table denotes that the actual carburization depth of the surface and opposite side is in agreement with the obtained ones. Therefore, it will be possible to detect the carburization depth of both surface and opposite side depth by using the proposed electromagnetic inspection method.

Table 1. Obtained results of the carburization depth of both the surface and the opposite in actual heating furnace steel tube

depth side	actual depth (mm)	inspection depth (mm)	error (mm)
surface (d_s)	0.91	1.00	0.09
opposite (d_o)	0.64	0.63	0.01
surface (d_s)	1.00	0.99	0.01
opposite (d_o)	1.87	1.86	0.01
surface (d_s)	0.96	0.95	0.01
opposite (d_o)	1.50	1.55	0.05
surface (d_s)	1.16	1.06	0.10
opposite (d_o)	1.72	1.60	0.12
surface (d_s)	1.45	1.50	0.05
opposite (d_o)	1.91	2.07	0.16

5 Conclusions

The results obtained by this research are summarized as follows:

(1) The permeability in the steel tube of the material STFA26 is decreased by the carburization. The maximum relative permeability in the steel tube without carburization is about 3.3 times of the steel tube with carburization. And the conductivity in the steel tube is decreased with the carburization. The conductivity of the steel without carburization is 1.28 times of the steel with carburization.
(2) The leakage flux on surface of steel tube is increased using alternating magnetic field of 500 Hz when the surface carburization depth is increased, since the permeability of carburization layer is lower than the non-carburization layer. Then, the leakage flux is increased using alternating magnetic field of 15 Hz when the opposite depth is increased, since the flux density is distributed in surface steel tube when the opposite side carburization depth with the low permeability domain is increased. Therefore, the non-contacting inspection of the carburization depth of both surface and opposite side steel tube is possible by detecting the rate of the change of leakage flux in a search coil.
(3) It is possible to estimate the carburization depth of both the surface and the opposite side in steel plate by the two kinds of exciting frequency using one proposed inspection sensor. Moreover, the calculated results using the 3-D nonlinear FEM are in agreement with the measured values using actual steel tube in an oil-refining plant.

References

1. Kamada, Y., Takahashi, S., Kikuchi, H., Kobayashi, S., Ara, K., Echigoya, J., Tozawa, Y., Watanabe, K.: Effect of predeformation on the precipitation process and magnetic properties of Fe-Cu model alloys. J. Mater. Sci. **44**, 949–953 (2009)
2. McMaster, R.C., Mclntrire, P., Mester, M.L.: "Electromagnetic Testing", Nondestructive Testing Handbook, vol. 5, 3rd edn. American Society for Nondestructive Testing, Columbus (2004)
3. Gotoh, Y., Sasaguri, N., Takahashi, N.: Evaluation of electromagnetic inspection of hardened depth of spheroidal graphite cast iron using 3-D nonlinear FEM. IEEE Trans. Magn. **46**(8), 3137–3144 (2010)
4. Gotoh, Y., Matsuoka, A., Takahashi, N.: Measurement of thickness of nickel-layer on steel using electromagnetic method. IEEE Trans. Magn. **43**(6), 2752–2754 (2007)
5. Gotoh, Y., Matsuoka, A., Takahashi, N.: Electromagnetic inspection technique of thickness of nickel-layer on steel plate without influence of lift-off between steel and inspection probe. IEEE Trans. Magn. **47**(5), 950–953 (2011)
6. Nakata, T., Kawase, Y., Nakano, N.: Improvement of measuring accuracy of magnetic field strength in single sheet testers by using two H coils. IEEE Trans. Magn. **23**(5), 2596–2598 (1987)